# Macular nerve fibre and ganglion cell layer changes in acute Leber's hereditary optic neuropathy

Nicole Balducci,[1] Giacomo Savini,[2] Maria Lucia Cascavilla,[3] Chiara La Morgia,[4,5] Giacinto Triolo,[3] Rosa Giglio,[3] Michele Carbonelli,[4] Vincenzo Parisi,[2] Alfredo A Sadun,[6,7] Francesco Bandello,[3] Valerio Carelli,[4,5] Piero Barboni[1,3]

▶ Additional material is published online only. To view please visit the journal online (http://dx.doi.org/10.1136/bjophthalmol-2015-307326).

[1]Studio Oculistico d'Azeglio, Bologna, Italy
[2]GB Bietti Foundation, Rome, Italy
[3]Scientific Institute San Raffaele, Milan, Italy
[4]IRCCS Institute of Neurological Sciences of Bologna, Bellaria Hospital, Bologna, Italy
[5]Unit of Neurology, Department of Biomedical and Neuromotor Sciences (DIBINEM), University of Bologna, Bologna, Italy
[6]Department of Ophthalmology, David Geffen School of Medicine at UCLA, Los Angeles, CA, USA
[7]Doheny Eye Institute, Los Angeles, CA, USA

**Correspondence to**
Dr Nicole Balducci, Studio Oculistico d'Azeglio, Via d'Azeglio, 5 Bologna 40123, Italy; balduccinicole@gmail.com

Received 15 June 2015
Revised 21 October 2015
Accepted 8 November 2015
Published Online First 27 November 2015

## ABSTRACT

**Aims** To evaluate longitudinal retinal ganglion cell inner plexiform layer (GC-IPL) and macular retinal nerve fibre layer (mRNFL) thickness changes in acute Leber's hereditary optic neuropathy (LHON).

**Methods** Six eyes of four patients with LHON underwent SD-OCT (optical coherence tomography) at month 1, 3, 6 and 12 after visual loss. In two eyes, the examination was carried out in the presymptomatic stage. The relationship and curves for area under the receiver operator characteristic (AUROC) were generated to assess the ability of each parameter to detect ganglion cell loss.

**Results** Significant longitudinal thinning of GC-IPL and mRNFL was detected in LHON. GC-IPL thinning was detectable in the deviation map during the presymptomatic stage in the inner ring of the nasal sector and then it progressively extended following a centrifugal and spiral pattern. Similarly, mRNFL thinning began in the inferonasal sector and it progressively extended. No further statistically significant changes were detected after month 3. The highest level of AUROC values at 1 month were detected in the nasal sectors and inferonasal mRNFL thickness reached AUROC value=1. All the parameters were equally able to detect ganglion cell loss from month 2 to 12.

**Conclusions** The natural history of GC-IPL thinning follows a specific pattern of reduction, reflecting the anatomical course of papillomacular fibres. Month 6 represents the end of GC-IPL loss. GC-IPL and mRNFL thinning is detectable before onset of visual loss. These observations can help future therapeutic approaches for both LHON carriers at high risk of conversion and patients with acute early LHON.

## INTRODUCTION

Leber's hereditary optic neuropathy (LHON) is a subacute neurodegenerative blinding disorder characterised by selective loss of retinal ganglion cells (RGCs), in particular those originating from small axons from the macula.[1 2] The primary cause of neurodegeneration is mitochondrial dysfunction due to maternally inherited mitochondrial DNA (mtDNA) point mutations affecting complex I subunit genes.[3] There are several puzzling features, such as male prevalence and incomplete penetrance. In fact, besides the mtDNA mutations, other factors may trigger the disease, such as mtDNA background, other still unknown nuclear genetic modifiers, and especially, environmental exposures including tobacco and alcohol consumption.[3–5]

Clinically, the disease is characterised by a presymptomatic stage with typical funduscopic changes including swelling of the peripapillary retinal nerve fibre layer (RNFL) and microangiopathy.[6 7] Conversion to the acute stage is defined by decline of visual acuity (VA) that rapidly worsens over several weeks. The central scotoma enlarges over a few months, usually reaching a stable and profound defect within a year, leading to the transition to the chronic stage.[6–8] Some patients may undergo spontaneous or treatment-related recovery that is usually of modest degree and affects various visual functions and with different timings.[1 9]

Major advancements in understanding LHON were possible after the introduction of optical coherence tomography (OCT). In fact, the natural history of peripapillary RNFL (pRNFL) changes in acute LHON has been quantitatively described.[10] The pRNFL thickness follows a specific pattern of early thickening and late thinning. This makes the cross-sectional analysis of RNFL thickness in LHON problematic as it may consist of opposite components of swelling and atrophy superimposed. The temporal and inferior quadrants show the earliest involvement of swelling, whereas the superior and nasal quadrants are affected later on and reveal their maximum thickness 3 months after the disease onset, when the papillomacular bundle is already atrophic. The RNFL swelling (pseudoedema) is likely to depend on the compensatory increase of mitochondrial biogenesis and/or axonal stasis along the fibres, and this does not allow detection of optic nerve atrophy in the early stages of the disease. Atrophic evolution of LHON may be better mirrored by RGC analysis of the macula, because in this area the influence of pRNFL and vessels can be avoided by investigating the RGC layer only.

An accurate and reproducible analysis of retinal ganglion cell and inner plexiform layer (GC-IPL) thickness is possible using the Cirrus HD-OCT ganglion cell analysis algorithm.[11–13] Moreover, retinal segmentation on the same macular sectors, provided by specific software, allows the analysis of other retinal layer thickness, including macular RNFL (mRNFL).[14]

To date, only one paper[15] and one case report[16] investigated the GC-IPL thickness in patients with LHON.

In this study we aimed at describing the presymptomatic and acute longitudinal changes of the GC-IPL and mRNFL thickness in patients with LHON and define the natural history of RGCs and mRNFL loss.

**To cite:** Balducci N, Savini G, Cascavilla ML, *et al*. *Br J Ophthalmol* 2016;**100**:1232–1237.

## METHODS

All patients included in the present study had a molecularly confirmed diagnosis of LHON (three patients had 11778/ND4 mutation and one patient had 3460/ND1). Six eyes of four consecutive patients (mean age: 20±7.35 years, range: 16–31 years, male:female=3:1) from four unrelated pedigrees were recruited with the inclusion criterion of being within the first month following onset of visual loss. Only one eye was included in two patients, as visual loss had begun more than 1 month earlier in the fellow eye. In the other two patients, the fellow asymptomatic eyes had a follow-up and when visual loss occurred these eyes were subsequently included in the analysis. All subjects had an extensive ophthalmologic examination, including best-corrected VA measurement, slit lamp biomicroscopy, intraocular pressure measurement, indirect ophthalmoscopy, and optic nerve head photography. Exclusion criteria were the presence of any retinal pathology and/or optic nerve disease other than LHON. All participants gave their informed consent according to the Declaration of Helsinki and the study was approved by the internal review board at the Department of Neurological Sciences, University of Bologna.

The control group was composed of 11 eyes of 6 subjects, matching the patient group for age, sex and axial length because the latter factor has been shown to influence peripapillary RNFL thickness as measured by Cirrus HD-OCT.[17 18] Age has also been shown to influence the macular GC-IPL thickness.[11]

All subjects underwent simultaneous macular GC-IPL and mRNFL thickness measurements by SD-OCT (Cirrus HD-OCT, software V.6.0; Carl Zeiss Meditec, Inc, Dublin, California, USA). All scans were acquired by the same operator, using the Macular Cube 512×128 protocols in eyes without pupil dilatation, as previously described.[19] Retinal segmentation was carried out according to the technique described by Saidha *et al*[14] using specific software provided by Carl Zeiss Meditec. Segmentation undertaken in three dimensions identified the outer boundary of the mRNFL, the outer boundary of the inner plexiform layer (IPL), and the outer boundary of the outer plexiform layer (OPL). Only high-quality scans, defined as scans with signal strength ≥7, without RNFL discontinuity or misalignment, involuntary saccadic or blinking artefacts, and absence of algorithm segmentation failure on careful visual inspection, were used for analysis. For GC-IPL and mRNFL, average and sectorial (superotemporal, superior, superonasal, inferonasal, inferior and inferotemporal) thicknesses were analysed.

Because of the small sample size, the data were analysed by non-parametric tests. Friedmann test with post-test was used to compare longitudinal GC-IPL and mRNFL thickness measurements during the follow-up period of the patients with LHON. Presymptomatic and 12-month results were not included in the statistical analysis because only two and four eyes respectively were available at that time and the data could not be paired. Mann–Whitney test was performed to compare GC-IPL and mRNFL thickness of patients with LHON and control subjects.

The relationship and curves for the area under the receiver operator characteristic (AUROC) were also generated to assess the ability of each parameter to detect GCL. Moreover, the AUROC curves were compared to test the equality in the AUROC using the DeLong method, as previously described.[20]

Statistical significance was assumed for p values <0.05. GraphPad Instat (V.3a) for Macintosh (GraphPad Software, San Diego, California, USA) and MedCalc V.13.0.4.0 (MedCalc, Mariakerke, Belgium) were used for statistical analysis.

## RESULTS

Four patients with bilateral LHON were enrolled. Two eyes were excluded because more than 1 month had elapsed from onset of visual loss. The remaining six eyes were followed up during the acute phase within 1 month of visual loss. Moreover, two eyes were analysed 6 weeks before visual loss (presymptomatic stage) because they were already being followed up for the fellow eye. Examinations were carried out at 1, 2, 3, 6 and 12 months. The last follow-up examination was performed in four eyes of three patients.

### GC-IPL changes from presymptomatic to symptomatic stage

In the two presymptomatic eyes, GC-IPL was assessed starting from 6 weeks prior to onset of visual loss. In both cases, the earliest sign was a thinning of the inner ring of the nasal sectors (figure 1). This defect progressively extended to the inner ring of the inferior sector and enlarged to the outer ring of the nasal sectors over a period of 1 month. Only at this stage did loss of VA occur. Later, the inner ring of the temporal and superior sectors became involved and subsequently the outer ring of the temporal sectors. This progression strictly reflects the anatomical distribution of papillomacular fibres. Finally, the outer ring of the superior and inferior sectors also underwent GC-IPL thinning (figure 2).

### GC-IPL analysis

Table 1 shows median and SD of average and sectorial macular GC-IPL thickness. Significant reduction of GC-IPL thickness occurred during the follow-up period. Post tests did not reveal statistically significant reductions by pairing two consecutive visits for each follow-up point, but revealed statistically significant reductions between the first and the third months in superotemporal, superior and superonasal sectors, and between the first and sixth months in all sectors.

Overall, the greatest GC-IPL thickness variation was detected between the presymptomatic stage and 1 month (−11.05%) and between the second and the third months after onset of visual loss (−11.62%), as reported in online supplementary table S2. The GC-IPL thickness reduction continued slowly until month 6 (−7.51%), with a minimal further reduction up to month 12

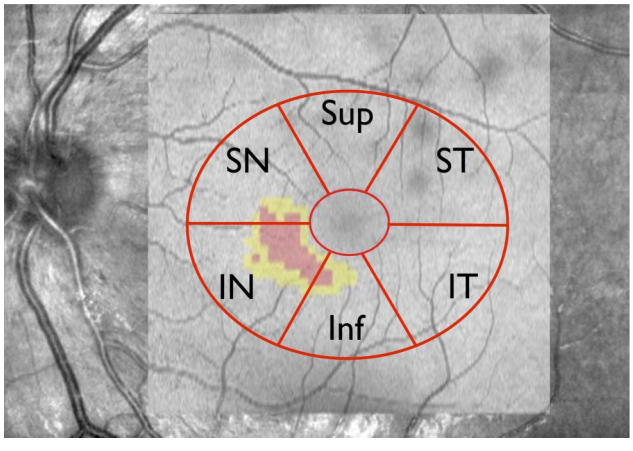


**Figure 1** Sectorial map superimposed on a deviation map in a patient with Leber's hereditary optic neuropathy analysed 6 weeks before visual loss onset. Note that the deviation map detects a localised defect in the inner ring of the inferonasal sector (IN, inferonasal; Inf, inferior; IT, inferotemporal; SN, superonasal; Sup, superior; ST, superotemporal).

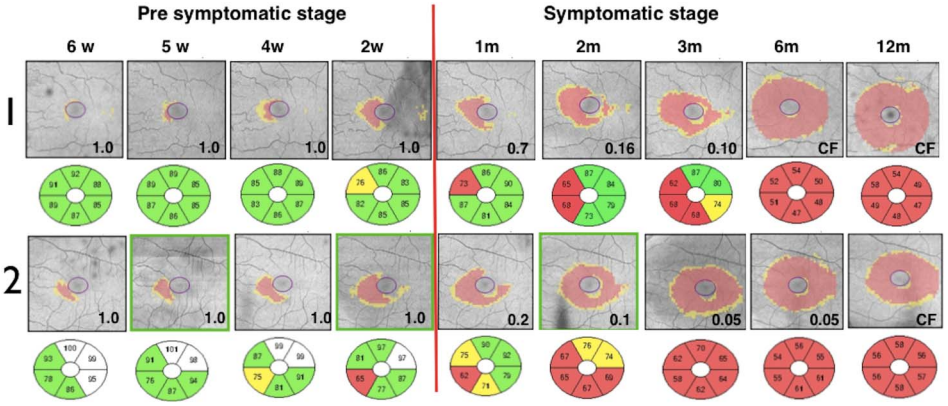


**Figure 2** Deviation and sectorial maps of two patients affected by Leber's hereditary optic neuropathy and followed before onset of visual loss. Note the similar early nasal thinning detected in the deviation map during the presymptomatic stage and its progression in a centrifugal and spiral pattern resembling the anatomic distribution of the papillomacular bundle fibres (m, months after onset of visual loss; w, weeks before onset of visual loss).

(−2.03%). Moreover, in the symptomatic stage, the GC-IPL variation thickness was more evident in the superior (−13.47%) and superotemporal (−14.99%) sectors rather than in the inferonasal, superonasal and inferior sectors, where GC-IPL thickness reduction began during the presymptomatic stage (−11.38% inferonasal, −20.65% superonasal and −12.72% inferior sectors respectively). Further reductions during the symptomatic phase were less pronounced.

GC-IPL thickness was lower in patients with LHON compared with control subjects during each visit and for each sector, with the exception of the superotemporal and superior sectors at month 1 (see online supplementary table S3).

### Macular RNFL analysis

Table 2 shows median and SD of average and sectorial mRNFL thickness. The Friedman test demonstrated significant thinning during the follow-up period for all the variables. Post tests did not reveal statistically significant reduction by pairing two consecutive visits for each follow-up point, but revealed statistically significant reductions between the first and the third months in average, superonasal, inferior and inferotemporal sectors, and between the first and sixth months in all sectors.

Overall, the greatest mRNFL thickness variation (−25.23%) was detected between months 2 and 3 after onset of visual loss (see online supplementary material table S5), but it was pronounced also between months 3 and 6 (−19.93%) and it continued until the last visit (−7.59%).

Moreover, the mRNFL thickness variation was more evident in the superior and superonasal sectors between months 2 and 3 (−31.55% and −32.08% respectively). By contrast, in the presymptomatic stage, mRNFL thickness variation was more evident in the inferonasal sector (−34.67%) and no variations were detected in the inferior and inferotemporal sectors. Subsequently, the inferonasal sector was the only sector where no further mRNFL thickness reduction was detected between 6 and 12 months.

Macular RNFL thickness was significantly reduced in patients with LHON compared with controls during each visit and for each sector, except for the inferior sector at month 1 and for the superotemporal and superior sectors at months 1 and 2 (see online supplementary material table S6).

Figure 3 summarises the most significant longitudinal variations that occurred in the two patients followed from the presymptomatic stage.

### AUROC curves

The AUROC curves at months 1 and 2 are reported in table 3, whereas the measurements at months 3, 6 and 12 were equally sensitive (AUROC=1).

At month 1, among all of the GC-IPL parameters, the superonasal and inferonasal sectors had the highest AUROC curves, whereas the superotemporal and the superior sectors had the lowest ones. At month 1, among all of the mRNFL parameters the superonasal and inferonasal sectors had the highest AUROC curves, while the superior and inferotemporal sectors had the lowest ones. Only the inferonasal mRNFL thickness had AUROC=1 at month 1.

No differences were detected when the AUROC curves of the GC-IPL and each corresponding mRNFL parameter were compared.

**Table 1** Ganglion cell inner plexiform layer thickness in patients with Leber's hereditary optic neuropathy over 1 year symptomatic stage

| | 1 month | 2 months | 3 months | 6 months | 12 months* |
|---|---|---|---|---|---|
| Average | 77.5±5.14 | 69.5±5.89 | 63.0±4.02 | 57.5±3.73† | 56.5±2.87 |
| Superotemporal | 84.0±9.95 | 74.5±6.89 | 64.0±4.89‡ | 54.0±4.72† | 53.0±4.08 |
| Superior | 87.0±5.80 | 75.0±8.32 | 64.0±5.98‡ | 55.0±3.92† | 56.5±2.08 |
| Superonasal | 73.0±4.81 | 66.5±5.61 | 61.5±4.82‡ | 55.5±5.42‡ | 57.5±2.87 |
| Inferonasal | 73.0±9.52 | 65.0±4.17 | 57.0±4.54 | 57.0±4.18‡ | 55.5±4.35 |
| Inferior | 73.5±5.68 | 68.0±6.37 | 61.0±4.55 | 57.5±5.56§ | 56.5±4.83 |
| Inferotemporal | 77.0±7.18 | 69.0±6.02 | 63.0±4.93 | 57.0±4.17† | 55.5±5.25 |

Median±SD thickness values, expressed in μm of average and sectorial GC-IPL (ganglion cells and inner plessiform layer) during the different examinations.
Friedman test with post test: p<0.0001 for average, superotemporal and superior sectors; p<0.01 for superonasal, inferonasal, inferior and inferotemporal sectors.
*Data not included in the statistical analysis.
†p<0.001 when compared with 1 month visit.
‡p<0.5 when compared with 1 month visit.
§p<0.01 when compared with 1 month visit.

**Table 2** Macular retinal nerve fibre layer (mRNFL) thickness in patients with Leber's hereditary optic neuropathy over 1 year symptomatic stage

| | 1 month | 2 months | 3 months | 6 months | 12 months* |
|---|---|---|---|---|---|
| Average | 29.5±5.64 | 24.5±6.12 | 17.0±4.24† | 14.5±1.37‡ | 13.0±3.70 |
| Superotemporal | 21.5±2.34 | 20.0±4.31 | 15.0±2.90 | 14.0±2.71† | 10.0±2.87 |
| Superior | 38.0±8.54 | 31.0±7.05 | 20.5±6.28 | 16.0±2.14† | 13.5±3.92 |
| Superonasal | 32.5±6.38 | 25.0±7.79 | 17.5±4.63† | 15.0±1.72‡ | 13.0±3.83 |
| Inferonasal | 24.5±7.56 | 23.0±8.34 | 18.0±4.50 | 14.0±2.42 | 14.5±3.51 |
| Inferior | 35.5±7.72 | 25.5±7.55 | 20.0±7.79† | 14.5±3.31‡ | 13.5±4.69 |
| Inferotemporal | 24.5±3.74 | 18.5±3.76 | 16.5±2.76† | 12.5±3.06‡ | 10.0±4.50 |

Median±SD thickness values, expressed in μm of average and sectorial mRNFL during the different examinations.
Friedman test with post test: p<0.01 for all the sectors, except for average and superior sector (p<0.001)
*Data not included in the statistical analysis.
†p<0.5 when compared with 1 month visit.
‡p<0.01 when compared with 1 month visit.

Moreover, the DeLong comparison of AUROC curves of each GC-IPL parameter with respect to each other at month 1 showed significant differences between inferior and nasals sectors versus superior and superotemporal sectors. The same comparison of mRNFL parameters demonstrated significant differences between inferior and nasal sectors versus superior and temporal sectors.

No differences were detected at month 2.

## DISCUSSION

This study presents longitudinal GC-IPL and mRNFL thickness changes during the early stages of LHON. We analysed six eyes from four patients: four eyes were followed within 1 month from visual loss and two eyes from the 'relative' presymptomatic phase. In fact, in these two patients the fellow eyes ware already involved. This analysis allowed detection of early GC-IPL and mRNFL damage.

Strikingly, early GC-IPL damage begins about 6 weeks before the onset of visual loss in patients with first eye involvement. As demonstrated in figure 1, GC-IPL thickness reduction begins in the inner ring of nasal sectors, where the RGC bodies that contribute to the papillomacular bundle fibres are contained. These results confirm the early and preferential involvement of the small axons of the papillomacular bundle in LHON.[6 21–22] Subsequently, the progression of loss extended as follows: inner ring of inferior sector, outer ring of the nasal sectors, inner ring of the temporal and the superior sectors, outer ring of the temporal sectors, outer ring of the superior and inferior sectors (figure 2). Thus, the progressive reduction of the GC-IPL thickness followed a centrifugal and spiral pattern resembling the anatomic distribution of the papillomacular bundle fibres.

This result confirms a recent study[23] evaluating total macular thickness in patients with LHON, stratified in five subgroups based on disease duration. The authors separately analysed the inner and the outer ring in nine different sectors with methodology corresponding to the Early Treatment Diabetic Retinopathy Study. We further demonstrate in this prospective and longitudinal study that macular thickness reduction is related to GC-IPL and mRNFL thickness reduction.

Moreover, we demonstrate that in the presymptomatic stage only the GC-IPL deviation map and not the sector analysis provided by Cirrus software can detect the early damage (figure 2). In fact, the sector analysis is not able to detect separately GC-IPL and mRNFL thickness of the inner and the outer rings of macular sectors. Thus, during the presymptomatic stage it is important to consider the defects detected in the deviation map,

**Table 3** Area under the receiver operator characteristic (AUROC) curves to detect ganglion cell loss at 1 and 2 months

| | 1 month | | | 2 month | | |
|---|---|---|---|---|---|---|
| Parameter | AUROC | SE | 95% CI | AUROC | SE | 95% CI |
| GC-IPL avg | 0.8409 | $0.098_{a}$ | 0.6497 to 1.032 | 1.000 | 0.000 | 0.805 to 1.000 |
| GC-IPL s-t | 0.5152 | $0.158_{b,c,d,e}$ | 0.2190 to 0.8113 | 0.886 | 0.086 | 0.641 to 0.987 |
| GC-IPL s | 0.5909 | $0.149_{c,d,e}$ | 0.3091 to 0.8727 | 0.939 | 0.065 | 0.711 to 0.998 |
| GC-IPL s-n | 0.9545 | $0.051_{a,f}$ | 0.8538 to 1.055 | 1.000 | 0.000 | 0.805 to 1.000 |
| GC-IPL i-n | 0.9091 | $0.094_{a,f}$ | 0.7334 to 1.085 | 1.000 | 0.000 | 0.805 to 1.000 |
| GC-IPL i | 0.8788 | $0.084_{a,f}$ | 0.7134 to 1.044 | 0.955 | 0.044 | 0.732 to 1.000 |
| GC-IPL i-t | 0.8333 | 0.105 | 0.6303 to 1.036 | 0.970 | 0.036 | 0.755 to 1.000 |
| mRNFL avg | 0.8712 | $0.103_{f,g}$ | 0.6741 to 1.068 | 1.000 | 0.000 | 0.805 to 1.000 |
| mRNFL s-t | 0.7424 | $0.127_{d}$ | 0.4976 to 0.9873 | 0.750 | 0.141 | 0.486 to 0.924 |
| mRNFL s | 0.6136 | $0.157_{b,c,d}$ | 0.3198 to 0.9075 | 0.765 | 0.129 | 0.501 to 0.932 |
| mRNFL s-n | 0.8788 | $0.090_{f,g}$ | 0.7046 to 1.053 | 1.000 | 0.000 | 0.805 to 1.000 |
| mRNFL i-n | 1.000 | $0.000_{a,f,g}$ | 0.8050 to 1.000 | 1.000 | 0.000 | 0.805 to 1.000 |
| mRNFL i | 0.7803 | $0.123_{g}$ | 0.5471 to 1.014 | 0.955 | 0.043 | 0.732 to 1.000 |
| mRNFL i-t | 0.5909 | $0.173_{b,c,d,e}$ | 0.2718 to 0.9100 | 0.864 | 0.099 | 0.613 to 0.979 |

Statistically significant versus: (a) s-t; (b) avg; (c) s-n; (d) i-n; (e) i; (f) s; (g) i-t.
avg, average; GC-IPL, ganglion cell inner plexiform layer; i, inferior; i-n, inferonasal; i-t, inferotemporal; mRNFL, macular retinal nerve fibre layer thickness; s, superior; SE, SE (DeLong analysis); s-n, superonasal; s-t, superotemporal.

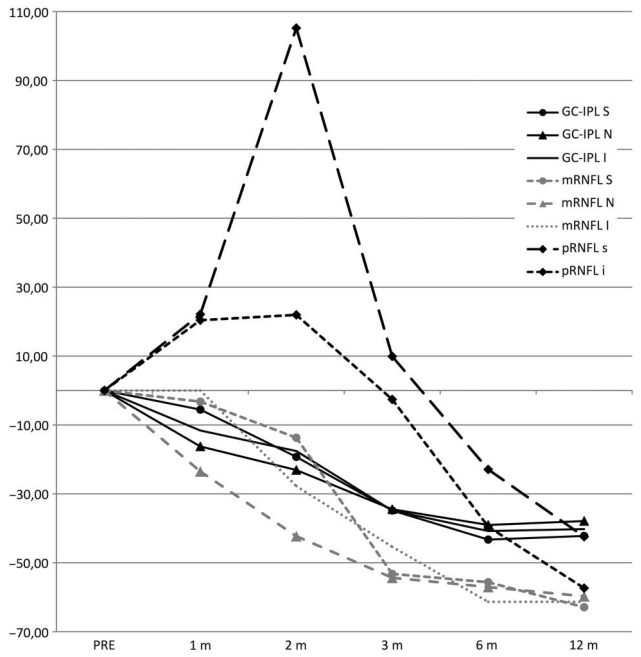


**Figure 3** Longitudinal thickness variations in different sectors observed in the two patients followed from the presymptomatic stage. Thickness variation is expressed as percentage (%) of reduction in respect to the presymptomatic examination. Note the different natural history of pRNFL, which shows early thickening and late thinning, in comparison to the early GC-IPL and mRNFL thickness reduction. Moreover, note the early involvement of nasal sectors for GC-IPL and mRNFL compared with the other sectors and the stability of GC-IPL thinning after 6 months compared with mRNFL and mostly pRNFL thinning, which continues until month 12. GC-IPL, ganglion cell inner plexiform layer; i, inferior quadrant; I, mean values of inferior and inferotemporal sectors; m, months after visual loss onset; mRNFL, macular retinal nerve fibre layer; N, mean values of inferonasal and superonasal sectors; PRE, presymptomatic stage (6 weeks); pRNFL, peripapillar retinal nerve fibre layer; s, superior quandrant; S, mean values of superior and superotemporal sectors.

particularly if they show an inner ring defect. This finding is in good agreement with previous studies on glaucomatous eyes, where deviation maps were shown to be more sensitive than clock-hour and quadrant maps when detecting pRNFL loss.[24] Thus, retinal anatomy trumps machine geometry.

The long interval of time between the macular GC-IPL thickness reduction and visual loss represents a window for detecting early disease conversion in carriers, which may be important in light of new therapeutic approaches.

Subsequently, no further significant thickness reduction of GC-IPL was detected after 6 months from visual loss, as recently reported[14] in a single case with 24-month follow-up. This observation has two important consequences: first, at 6 months we define the residual RGCs, which may predict visual prognosis years later; second, month 6 after onset represents the therapeutic window of opportunity for future clinical trials.

MRNFL thickness analysis demonstrates an early thinning of the nasal sectors between the presymptomatic stage and month 1 after disease onset (see online supplementary material table S5). As shown by the AUROC analysis (table 3) the earliest parameter that can clearly detect ganglion cell loss is the inferonasal mRNFL sector (AUROC=1 at month 1).

This may be because early nasal macular thinning is greater in mRNFL than in GC-IPL, and retinal nerve fibres, from the RGCs of the inner ring, run superficially and widely over the nasal sector from the fovea to the optic nerve, causing a diffuse thinning of nasal sectors and not a localised thinning, as seen in GC-IPL. Moreover, mRNFL thinning showed a trend of progression up to 1 year after visual loss, although these differences were not significant, suggesting that mRNFL analysis might be a preferable measurement for late stages of the disease.

In a previous study[10] we analysed pRNFL thickness changes in the early stage of LHON, which showed a specific pattern of early thickening and late thinning. Similarly, pRNFL thickness of patients with LHON enrolled in the present study followed the same specific pattern and the earliest pRNFL thinning is visible in the inferior and temporal quadrants that contain fibres of the papillomacular bundle. Correspondingly, the earliest GC-IPL and mRNFL thinning is detectable in the inferior and nasals sectors, so the current data confirm that the papillomacular bundle is primarily involved in LHON. Figure 3 reports the main significant longitudinal GC-IPL, mRNFL and pRNFL thickness variations that occurred in the two patients followed from the presymptomatic stage and clearly shows the dissociation between the early pRNFL thickening and the GC-IPL and mRNFL thinning.

The pRNFL swelling (pseudoedema) does not allow the detection of optic nerve atrophy in the early stages of the disease. Thus, in the presymptomatic and early stage of LHON, atrophic evolution is better represented by GC-IPL analysis of the macular sectors, which is less confounded by the influence of pRNFL and vessels. We propose that GC-IPL analysis can detect the optic nerve damage in patients with LHON earlier than pRNFL analysis. Instead, during the middle and late stages of the disease (3–12 month), mRNFL and pRNFL thickness provide the most reliable information about disease progression.

Our study is in agreement with that by Akiyama *et al*[15] who detected diffuse GC-IPL loss in four of six patients with LHON at the time of visual loss, before pRNFL thickness measurement could reveal any decrease. However, they did not describe longitudinal GC-IPL thickness changes in the early stages of the disease.

Limitations of the present study include, first, small sample size and the fact that only two patients were analysed during the presymptomatic stage. However, because patients with LHON are rarely observed before visual loss, we believe that this is a rare opportunity for describing the longitudinal changes of GC-IPL and mRNFL thickness. Second, we analysed both eyes in two patients and this approach can be problematic from a statistical point of view. However, the rarity of opportunity to examine patients with LHON with such a close follow-up in the earliest stages justifies the inclusion of both eyes.

The present study provides key corroboration of previous investigations[2 21–22] that reveal an important feature in the pathobiology of LHON. This diseases spreads as a wave, beginning with the involvement of the smallest calibre fibres found in the inferior portion of the papillomacular bundle. The pathology then progresses in the precise pattern predicted by a mathematical model[2 22] that captures the differential energy burden dictated by the cable properties of axons.

In conclusion, we demonstrate that GC-IPL and mRNFL analysis can detect early damage in the presymptomatic stage of LHON and may have an important prognostic value. This observation could be of crucial importance for future therapeutic approaches for LHON carriers at high risk of conversion and patients with early acute LHON.

**Contributors** NB: statistical analysis and interpretation, manuscript preparation. GS: data acquisition and data analysis. MLC: data acquisition. CLM: study design,

data interpretation, manuscript preparation. GT: data acquisition and research execution. RG: data acquisition, research execution. MC: data interpretation, manuscript preparation. VP: data interpretation. AAS: manuscript preparation, data interpretation. FB: data analysis and interpretation. VC: research design, data interpretation, manuscript preparation. PB: study design, data acquisition and research execution, data analysis and interpretation, manuscript preparation.

**Funding** Fondazione Bietti is supported by the Italian Ministry of Health and Fondazione Roma; IRCCS Istituto di Scienze Neurologiche di Bologna is supported by the Ministry of Health.

**Competing interests** None declared.

**Patient consent** Obtained.

**Ethics approval** Department of Neurological Sciences, Bologna, Italy.

**Provenance and peer review** Not commissioned; externally peer reviewed.

## REFERENCES

1 Carelli V, Ross-Cisneros FN, Sadun AA. Mitochondrial dysfunction as a cause of optic neuropathies. *Prog Retin Eye Res* 2004;23:53–89.
2 Sadun AA, La Morgia C, Carelli V. Mitochondrial optic neuropathies: our travels from bench to besides and back again. *Clin Experiment Ophthalmol* 2013;41:702–12.
3 Maresca A, Caporali L, Strobbe D, *et al*. Genetic basis of mitochondrial optic neuropathies. *Curr Mol Med* 2014;14:985–92.
4 Carelli V, Achilli A, Valentino ML, *et al*. Haplogroup effects and recombination of mitochondrial DNA: novel clues from the analysis of Leber hereditary optic neuropathy pedigrees. *Am J Hum Genet* 2006;78:564–74.
5 Kirkman MA, Yu-Wai-Man P, Korsten A, *et al*. Gene–environment interactions in Leber hereditary optic neuropathy. *Brain* 2009;132:2317–26.
6 Nikoskelainen E, Hoyt WF, Nummelin K. Ophthalmoscopic findings in Leber's hereditary optic neuropathy: II. The fundus findings in the affected family members. *Arch Ophthalmol* 1983;101:1059–68.
7 Nikoskelainen E, Hoyt WF, Nummelin K. Ophthalmoscopic findings in Leber's hereditary optic neuropathy. I. Fundus findings in asymptomatic family members. *Arch Ophthalmol* 1982;100:1597–602.
8 Riordan-Eva P, Sanders MD, Govan GG, *et al*. The clinical features of Leber's hereditary optic neuropathy defined by the presence of a pathogenic mitochondrial DNA mutation. *Brain* 1995;118:319–37.
9 La Morgia C, Carbonelli M, Barboni P, *et al*. Medical management of hereditary optic neuropathies. *Front Neurol* 2014;5:141.
10 Barboni P, Carbonelli M, Savini G, *et al*. Natural history of Leber's hereditary optic neuropathy: longitudinal analysis of the retinal nerve fiber layer by optical coherence tomography. *Ophthalmology* 2010;117:623–7.
11 Mwanza JC, Oakley JD, Budenz DL, *et al*. Macular ganglion cell-inner plexiform layer: automated detection and thickness reproducibility with spectral domain-optical coherence tomography in glaucoma. *Invest Ophthalmol Vis Sci* 2011;52:8323–9.
12 Kim KE, Yoo BW, Jeoung JW, *et al*. Long-term reproducibility of macular ganglion cell analysis in clinically stable glaucoma patients. *Invest Ophthalmol Vis Sci* 2015;56:4857–64.
13 Francoz M, Fenolland JR, Giraud JM, *et al*. Reproducibility of macular ganglion cell-inner plexiform layer thickness measurement with cirrus HD-OCT in normal, hypertensive and glaucomatous eyes. *Br J Ophthalmol* 2014;98:322–8.
14 Saidha S, Sotirchos ES, Ibrahim MA, *et al*. Microcystic macular oedema, thickness of the inner nuclear layer of the retina, and disease characteristics in multiple sclerosis: a retrospective study. *Lancet Neurol* 2012;11:963–72.
15 Akiyama H, Kashima T, Li D, *et al*. Retinal ganglion cell analysis in Leber's hereditary optic neuropathy. *Ophthalmology* 2013;120:1943–4.
16 Mizoguchi A, Hashimoto Y, Shinmei Y, *et al*. Macular thickness changes in a patient with Leber's hereditary optic neuropathy. *BMC Ophthalmol* 2015;15:27.
17 Knight OJ, Girkin CA, Budenz DL, *et al*. Effect of race, age, and axial length on optic nerve head parameters and retinal nerve fiber layer thickness measured by Cirrus HD-OCT. *Arch Ophthalmol* 2012;130:312–18.
18 Alasil T, Wang K, Keane PA, *et al*. Analysis of normal retinal nerve fiber layer thickness by age, sex and race using spectral domain optical coherence tomography. *J Glaucoma* 2013;22:532–41.
19 Barboni P, Savini G, Cascavilla ML, *et al*. Early macular retinal ganglion cell loss in dominant optic atrophy: genotype-phenotype correlation. *Am J Ophthalmol* 2014;158:628–36.
20 Gonul S, Koktekir BE, Bakbak B, *et al*. Comparison of ganglion cell complex and retinal nerve fibre layer measurements using Fourier domain optical coherence tomography to detect ganglion cell loss in non-arteritic anterior ischaemic optic neuropathy. *Br J Ophthalmol* 2013;97:1045–50.
21 Sadun AA, Win PH, Ross-Cisneros FN, *et al*. Leber's hereditary optic neuropathy differentially affects smaller axons in the optic nerve. *Trans Am Ophthalmol Soc* 2000;98:223–32.
22 Pan BX, Ross-Cisneros FN, Carelli V, *et al*. Mathematically modeling the involvement of axons in Leber's hereditrary optic neuropathy. *Invest Ophthalmol Vis Sci* 2012;53:7608–17.
23 Zhang Y, Huang H, Wei S, *et al*. Characterization of macular thickness changes in Leber's hereditary optic neuropathy by optical coherence tomography. *BMC Ophthalmol* 2014;14:105.
24 Kim NR, Lee ES, Seong GJ, *et al*. Spectral-domain optical coherence tomography for detection of localized retinal nerve fiber layer defects in patients with open-angle glaucoma. *Arch Ophthalmol* 2010;128:1121–8.

# Macular nerve fibre and ganglion cell layer changes in acute Leber's hereditary optic neuropathy

Nicole Balducci, Giacomo Savini, Maria Lucia Cascavilla, Chiara La Morgia, Giacinto Triolo, Rosa Giglio, Michele Carbonelli, Vincenzo Parisi, Alfredo A Sadun, Francesco Bandello, Valerio Carelli and Piero Barboni

*Br J Ophthalmol* 2016 100: 1232-1237 originally published online November 27, 2015
doi: 10.1136/bjophthalmol-2015-307326